Load capacity of stone columns and geosynthetic encased stone columns during and after seismic excitations

Cihan Cengiz[1]
[1] *Department of Civil Engineering, Bogazici University, Istanbul, Turkey, c.cihancengiz@gmail.com*

Erol Güler[2]
[2] *Department of Civil Engineering, Bogazici University, Istanbul, Turkey, eguler@boun.edu.tr*

Dimiter Alexiew[3]
[3] *HUESKER GmbH, Gescher, Germany, dalexiew@huesker.de*

KEYWORDS: Shaking table tests, geosynthetic encased stone columns, stone columns

ABSTRACT: Stone columns are often used to enhance the bearing capacity of weak soils. When such sites are in earthquake prone regions, determination of seismic performance of stone columns becomes imperative. In this study, settlement behaviors of conventional stone columns and geosynthetic encased stone columns (GECs) under seismic excitations are compared by model tests. The seismic excitations are applied on the models by making use of a 10 ton capacity shaking table. The vertical load capacities and vertical stress-strain behavior of model columns were also investigated. It is concluded that the geosynthetic encapsulated stone columns reduced the settlements under sustained load during the seismic excitation phase of the experimental program. GECs also exhibited higher load capacity during the pile load tests.

1 INTRODUCTION

Stone columns have been used in a wide spectrum of applications for the construction of various structures with rigid and flexible foundations. For situations when the undrained shear strength of soil is too weak, stone columns may lose their effectiveness as the surrounding weak soils may not provide enough confinement to the columns, which may result in bulging or crushing failure of the columns at the upper section of the columns (Hughes et al., 1975). In that case, a proper geosynthetic (typically geotextile) encasement helps to overcome the shortcomings of a conventional stone column providing lateral confinement to the granular column constituents to improve the bearing capacity of the soils (Raithel et al., 2005; Yoo, 2010; Zhang et al., 2012; Dash and Bora, 2013; Elsawy, 2013; Wu and Hong, 2014). The use of both stone columns and GECs have proven to be a viable ground modification technique owing to their simplicity in application which reduces the construction period and costs. While the primary function of the stone columns (and GECs) is to take vertical loads from the foundation and to transmit the load to the firm strata, there is also a secondary function , namely, to accelerate the drainage and thus the consolidation. . The literature about stone columns and GECs cover analytical models, finite elements models, and physical models. While there is an abundance of literature on the performance of stone columns and GECs under the action of static loads, there are not many studies addressing the engineering behaviour of stone columns and GECs subjected to dynamic loads such as earthquake excitations. Guler et. al. (2014) have studied the behaviour of GECs by running a time history analysis by utilizing DIANA numerical code.

In this study first preliminary findings of a broader shaking table testing scheme have been presented. The results presented here pertain to a singular model sized stone column and a GEC.

2 SAMPLE PREPARATION AND TEST PROCEDURE

In general the stone columns and geosynthetic encapsulated stone columns are implemented in soils which have a c_u value of 15 kPa or below. Due to the confining encasement there is practically no lower limit for GECs. In order to prepare a clay bed with $c_u < 15$ kPa, kaolinite clay was mixed with tap water at a water content of 75 %. The clay slurry was then placed into a large rigid box where it was consolidated and aged. The clay slurry was consolidated under an overburden pressure of 12 kPa. The rigid box that was used for the experiments had the following dimensions: Height 216 cm, width 52 cm, depth 220 cm. A sketch of the test setup is shown in Figure 1. At the base of the rigid box a sand layer is installed which is intended to provide drainage of the overlying clay. The clay is placed in a non-woven geotextile (500g/m^2) sack and the top portion of the geotextile is wrapped onto itself and glued in order to prevent clay slurry from leaking out in the early stages of consolidation. The overburden pressure is given to the sample by making use of four pneumatic pistons. The rods extending from the pneumatic pistons were fitted with perforated steel plates which were in direct contact with the geotextile sack's top portion which was used to contain the clay slurry. The inner part of the rigid box was fitted with EPS blocks on either side (in the front and the back of it) which were perpendicular to the direction of shaking. The reason for placing the EPS blocks was to prevent the seismic waves from traveling in a recurrent manner throughout the model. In other words, the sole purpose of the EPS blocks was to dampen the seismic waves travelling through the model so that they did not get reflected back to the model in an amplified manner. Cihan et. al. (2015) has shown that having no damping at the model boundary could cause the model to experience loads which are way beyond the magnitude of realistic load amplitudes. Such severe loading gives erratic results and may lead to conservative design approaches. Upon completion of consolidation, a closed-end casing pipe whose diameter was 168 mm was driven into the clay bed and model column constituents (gravel only for the case of the model stone columns and geotextile encasement and gravel for GECs) were placed in the hollow space. The pipe was retracted once the placement of the column constituents was completed.

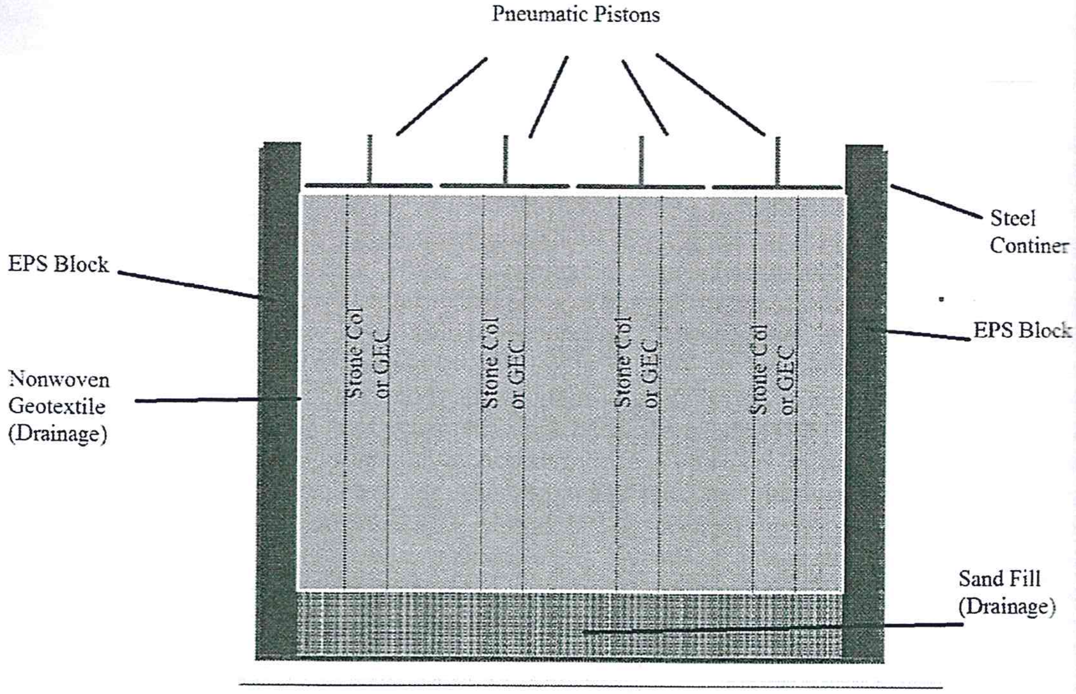

Figure 1. A sketch of the test setup

In order to quantify the strains occurring on the geosynthetic encasements, strain rosettes were applied on them. The strain rosettes were made use of instead of conventional strain gauges. The reason behind this was to be able to track the planar strain in the entire geosynthetic surface. An illustration of the strain rosettes used in this study is given in Figure 2. The centers' of the strain gauges in the first line and the third line from the top of the GEC is as follows: 140, 280, 420, 560, 750, 940, and 1130 mm. The centers of the strain gauges were determined as such in order to have redundant strain gauges in the event that the strain gauges were damaged. The data acquired from the gauges could be cross-checked. The strain gauges located on the second line (depicted in Figure 2) enabled the acquisition of the strain data at intermediate elevations of the GEC where first and third line strain gauges were not able to scan. Upon completion of the tests, a vane test was made to quantify the undrained shear strength of the clay bed. A total of four vertical arrays on the clay bed was tested and from each array vane readings were taken at various elevations (35, 65 90, and 120 cm below the top of the clay bed). The difference in the undrained shear strength can be explained by clay consolidating under its self-weight which gives rise to higher undrained shear strength reading as the vane probe is lowered.

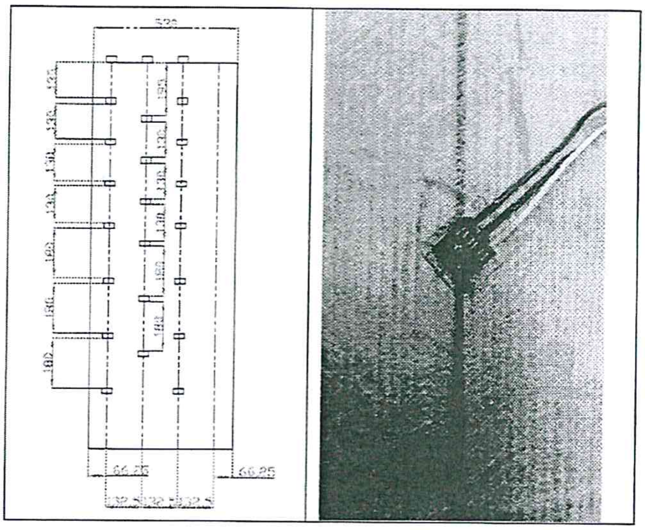

Figure 2. The positions of the strain gauges on the geotextile encasement before it was sewn (on the left), and a singular strain gauge (on the right)

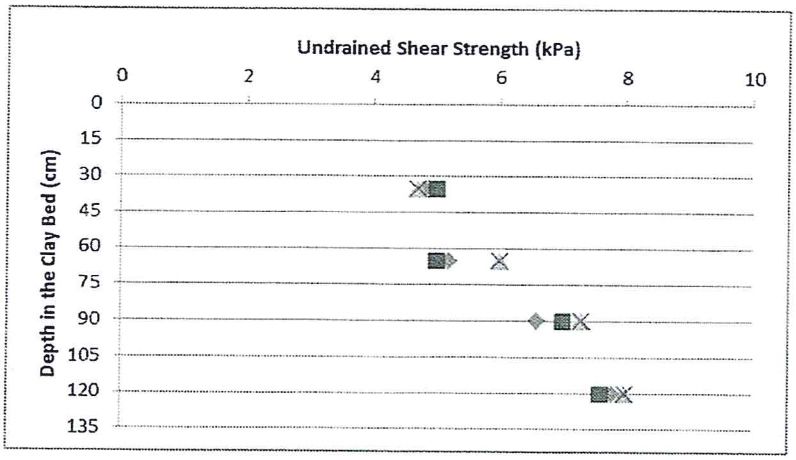

Figure 3. Undrained shear strength readings taken from the clay bed in the rigid box (different data markers indicate various vertical alignments that the vane probe was inserted to the clay bed)

3 SEISMIC EXCITATIONS AND FORCE CONTROLLED COLUMN TESTS

The test model, which was confined by the rigid box, was subjected to two different strong ground motion recordings. These recordings pertained to El-Centro (north-south component, PGA = 0.33 g) and Kobe (north-south component, PGA = 0.8 g) earthquakes. During the application of seismic excitations, pneumatic pistons were used to apply a constant surcharge load on the sand fill which was spread and compacted over the column heads. The height of the sand fill was 30 cm. Two laser displacement sensors were fitted to each pneumatic piston and settlement of the soil-column composite was monitored during testing. The test setup was allowed sufficient time between the application of seismic excitations so that the excess pore water pressures could dissipate. Upon completion of seismic excitations, the stone columns and GECs were subjected to a force controlled pile capacity tests where increments of vertical stress were applied to column heads. The columns were subjected to each load increment for 60 seconds and during this period settlement of the column head was recorded. Strain readings were also taken from GECs.

4 RESULTS AND DISCUSSION

The test setup was initially subjected to a scaled version of the El-Centro accelerogram. The response of the stone columns and GECs in the vertical direction was monitored as prescribed above. The settlement behavior of the stone column and the GEC under the action of imposed El Centro accelerogram is illustrated in Figure 4. The GEC has undergone a total settlement of 1.2 mm whereas its counterpart has undergone a total settlement of 1.7 mm which equates the settlement reduction achieved by GEC to **30 %** . The intensity of the El Centro earthquake excitation, as applied to the test setup, did not evoke significant amounts of settlement. Therefore comparison of settlement reduction might not reflect the prototype behavior objectively. During the Kobe earthquake excitation however, the difference in vertical settlements of the GEC and the stone column was more pronounced. The difference in settlement was about 5.5 mm and this equates the settlement reduction to **20 %.** The data illustrated in Figure 4 and 5 include the ambient vibration portions (zero pads) before and after the application of the input motion. By comparing the settlement differences before and after the seismic excitation, the plastic deformations that the columns have undergone could be computed. The zero pads have also been introduced to the data for further analysis of the acquired data when the data will be subjected to Fourier Transform (Fast Fourier Transform) to be analyzed in frequency domain. Since the amplitude of the settlement is relatively small in the data illustrated in Figure 4, the distortion or noise in the data is more pronounced. The data in Figure 5 on the other hand is seemingly more legible.

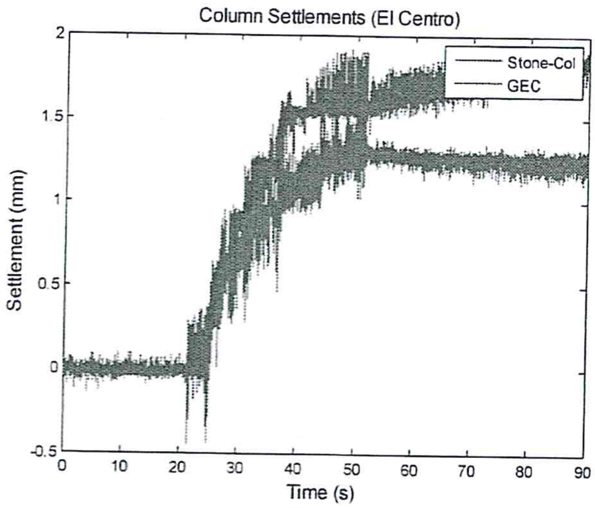

Figure 4. Settlement behavior of surcharge plates over GEC and stone column during El Centro input motion (green data series pertain to GEC)

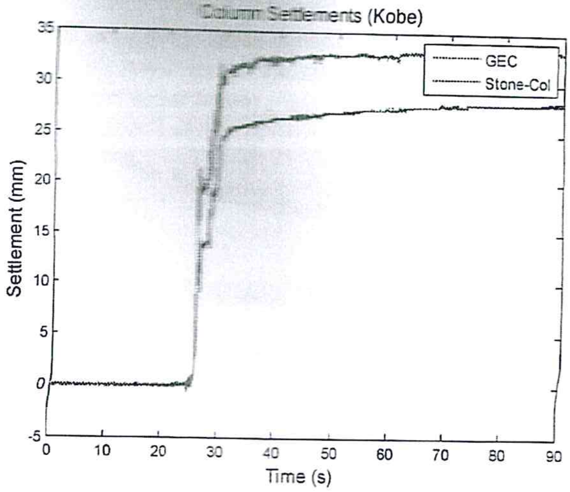

Figure 5. Settlement behavior of surcharge plates over GEC and stone column during Kobe input motion (blue data series pertain to GEC)

The geosynthetic reinforcement was monitored for the occurrence of strains in the entire testing program. The strain behavior that is illustrated in Figure 6 shows that the reinforcement has indeed functioned as expected during the seismic excitation. In Figure 6 a the strain readings from the strain gauge at an elevation of 280 mm from the pile head is illustrated, and in Figure 6 b, the input motion for El Centro earthquake is illustrated. In Figure 7, the strain data from the same strain gauge during the Kobe earthquake excitation is illustrated in a similar fashion to that of Figure 6. With assigned data acquisition settings, elongation of the geotextile corresponds to negative strain, and compression of the geotextile is manifested as positive strain. It is inferred that the bulging behavior of the GEC at the selected elevation has strained the reinforcement geotextile to elongate radially causing horizontal strains. The radial bulging and vertical load on the GEC has caused the vertical strains at the same location to be in compressive strains. The strain gauge designated as skew in Figures 6 and

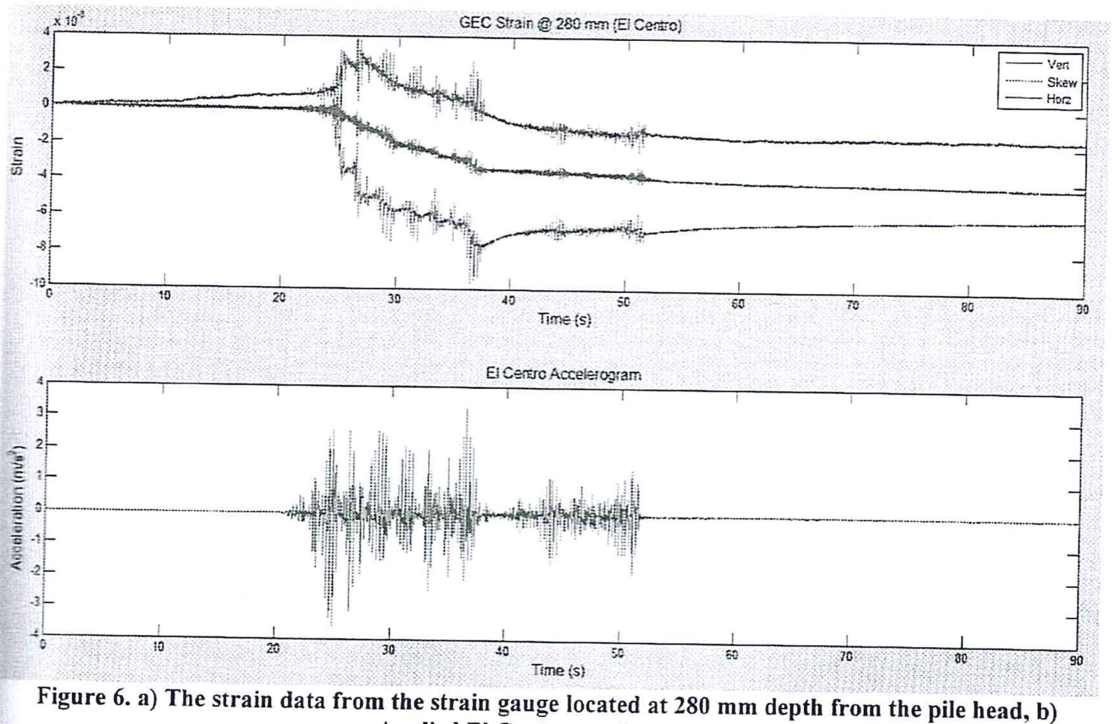

Figure 6. a) The strain data from the strain gauge located at 280 mm depth from the pile head, b) Applied El Centro accelerogram

7 pertain to the component of the strain gauge assembly (strain rosette) which mutually makes an angle of 45 degrees to both vertical and the horizontal strain gauge (as illustrated in Figure 2). The magnitude of strain changes drastically as the intensity of the input motion increases. The trend of the data in Figures 6 and 7 have a resemblance in the general trend but the amplitude of strains is at least ten times greater.

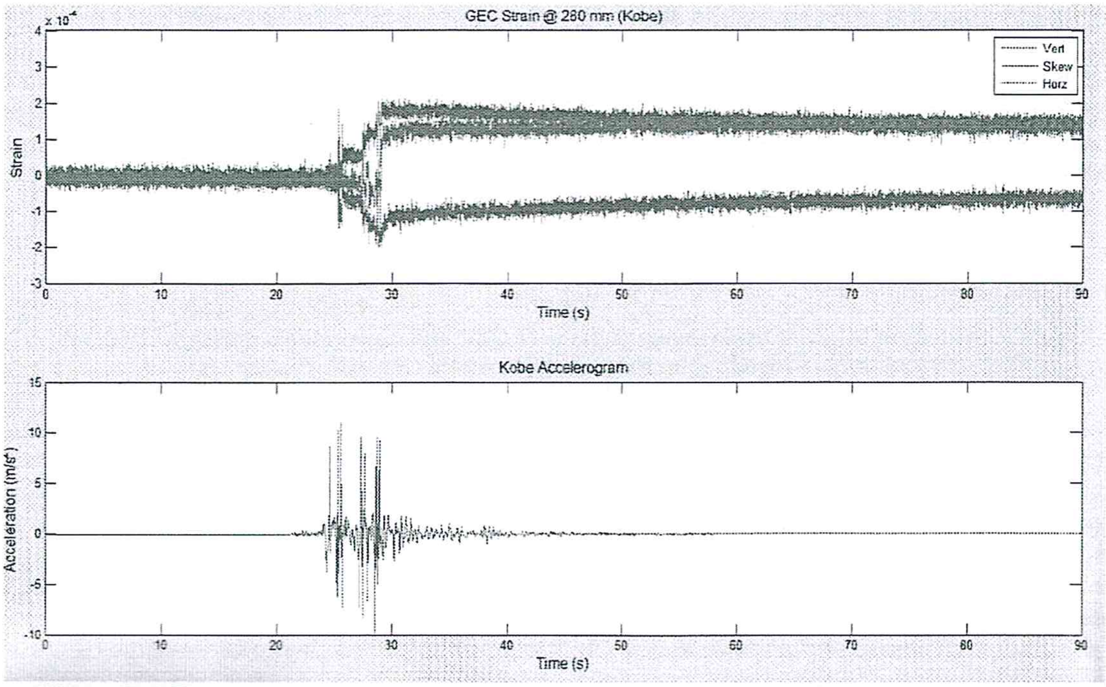

Figure 7. a) The strain data from the strain gauge located at 280 mm depth from the pile head, b) Applied Kobe accelerogram

In Figure 8, the data pertaining to the last stage of force controlled pile loading test data is presented. The sustained air pressure in the pneumatic piston is 350 kPa and the piston has an inner area of 0.02 m^2 which equates the applied load to roughly 7 kN. At this stage of loading which took place on a time period of 1 minute data was taken at 100 Hz. The time graph therefore reflects 1/100 second for

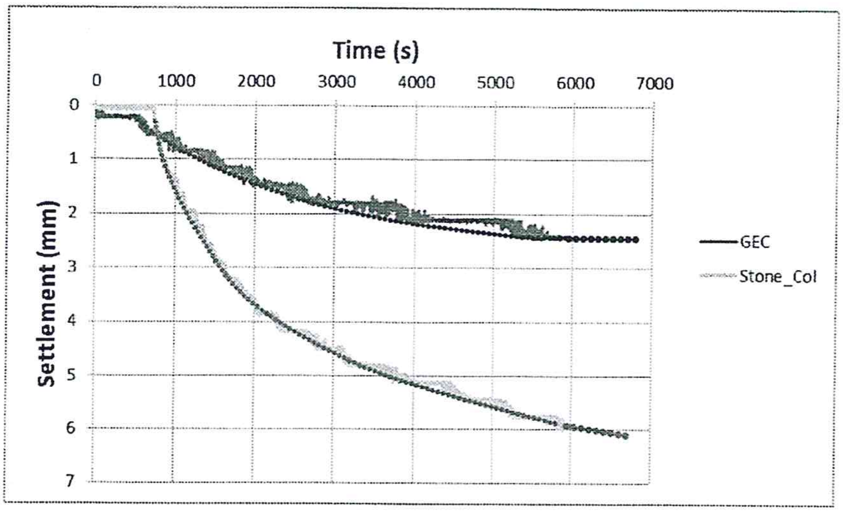

Figure 8 Post-dynamic load-settlement behavior of GEC and stone column in the last increment of loading (vertical load = 7 kN i.e. 350 kPa pressure)

every data point presented. Zero pads in other words the state of the columns before the application of the load is also displayed in the data (the initial flat portions of the graphs). From Figure 8, it is seen that the GEC undergoes a settlement that is 3 folds less than that of the conventional stone column. The post-dynamic loading settlement behavior of the GEC seems to be superior to the conventional stone column because the stone column has settled 6 mm in this increment of the force controlled test while the GEC settled a mere amount of 2 mm.

It is also important to be noted, that after 6000 s (about one and a half hours) after load application there is no more tendency of settlement increase for GEC; on the contrary, such a tendency is still existing for the non-encased stone column (Fig. 8, dotted trend lines).

6 CONCLUSIONS

Main conclusions drawn from the undertaken experimental analysis is listed below:

- GECs have shown a markedly better settlement reduction performance than the conventional stone columns under the action of the seismic excitations
- The geotextile encasement has behaved as expected. The strain amplitude has increased as the intensity of the impact increased.
- The geotextile encasement material has bulged horizontally (radially) while contracting vertically at the proximity of the top bulging zone of the GEC.
- Post-dynamic loading settlement performance of the GEC was significantly better to that of the stone column.

ACKNOWLEDGEMENTS

Authors gratefully acknowledge the financial support for this project provided by TUBITAK (Scientific and Technological Research Council of Turkey) under the project number 213M359.

REFERENCES

Cengiz, C., Kılıc, I. E., Guler, E. (2015) "Geosentetik Donatılı Taş Kolonlarla Desteklenen Bir Toprak Seddenin Farklı Sönümleme Modelleri ile Analizleri" 6. Adana Geoteknik Sempozyumu, (In Turkish).

Dash, S.K., Bora, M.C., 2013. Influence of geosynthetic encasement on the performance of stone columns floating in soft clay. Can. Geotech. J. 50 (7), 754-765.

Elsawy, M.B.D., 2013. Behaviour of soft ground improved by conventional and geogrid-encased stone columns, based on FEM study. Geosynth. Int. 20 (4), 276-285.

Guler, E., Alexiew, D., Abbaspur, A., Koc, M., "Seismic performance of geosynthetic encased stone columns", TRB 2014 Annual Meeting, Washington D.C., USA

Hughes, J.M.O., Withers, N.J., Greenwood, D.A., 1975. Afield trial of the reinforcing effect of a stone column in soil. Geotechnique 25 (1), 31-44.

Raithel, M., Kirchner, A., Schade, C., 2005. Foundation of constructions on very soft soils with geotextile encased columns -state of the art. In: Proceedings of GeoFrontiers 2005, Austin, Texas, USA, pp. 1-11.

Wu, C.S., Hong, Y.S., 2014. A simplified approach for evaluating the bearing performance of encased granular columns. Geotext. Geomemb. 42 (4), 339-347.

Yoo, C., 2010. Performance of geosynthetic-encased stone columns in embankment construction: numerical investigation. J. Geotech. Geoenviron. Eng. 136 (8), 1148-1160.

Zhang, Z., Han, J., Ye, G.B., 2014. Numerical investigation on factors for deep-seated slope stability of stone column-supported embankments over soft clay. Eng. Geol. 168, 104-11